5. E. M. Crouch *et al.*, *Geology* **29**, 315 (2001).
6. C. Robert, J. P. Kennett, *Geology* **22**, 211 (1994).
7. W. C. Clyde, P. D. Gingerich, *Geology* (1998).
8. J. P. Kennett, L. D. Stott, *Nature* **353**, 225 (1991).
9. J. Zachos, M. Pagani, L. Sloan, E. Thomas, K. Billups, *Science* **292**, 686 (2001).
10. E. Thomas, N. J. Shackleton, in *Correlation of the Early Paleogene in Northwest Europe,* R. W. O. B. Knox, R. M. Corfield, R. E. Dunay, Eds. (Geological Society of London, London, 1996), vol. 101, pp. 401–441.
11. G. R. Dickens, M. M. Castillo, J. C. G. Walker, *Geology* **25**, 259 (1997).
12. G. R. Dickens, J. R. O'Neil, D. K. Rea, R. M. Owen, *Paleoceanography* **10**, 965 (1995).
13. C. J. Shellito, L. C. Sloan, M. Huber, *Palaeogr. Palaeoclimatol. Palaeoecol.* **193**, 113 (2003).
14. V. A. Alexeev, *Clim. Dyn.* **20**, 775 (2003).
15. T. J. Bralower *et al.*, *Geology* **25**, 963 (1997).
16. L. D. Stott, *Paleoceanography* **7**, 395 (1992).
17. T. J. Bralower *et al.*, *Proceedings ODP, Initial Reports* (Ocean Drilling Program, College Station, TX, 2002), vol. 198.
18. D. J. Thomas, T. J. Bralower, J. C. Zachos, *Paleoceanography* **14**, 561 (1999).
19. S. D'Hondt, J. C. Zachos, G. Schultz, *Paleobiology* **20**, 391 (1994).
20. Stable isotope analyses were performed using an Autocarb preparation device coupled to a PRISM gas-source mass spectrometer. This common acid bath system reacts carbonates in phosphoric acid at 90°C. The CO_2 is distilled in a single step. Analytical precision for $\delta^{18}O$ and $\delta^{13}C$, based on replicate measurements of in-house standard, is ± 0.1 and $\pm 0.05‰$, respectively.
21. Before analysis, samples were crushed, weighed, and subjected to multiple sonication steps to remove fines, to reductive cleaning to remove oxyhydroxide coatings, to oxidative cleaning to remove organics, and to one partial acid dissolution in 0.001 N trace metal grade HNO_3. Finally, samples were dissolved in 0.5 N trace metal grade HNO_3 and analyzed within 6 hours. Measurements of Mg/Ca were made with a Perkin-Elmer Optima 8300 inductively coupled plasma optical emission spectrometer. We used a ratio intensity calibration method. Over the period during which the records at Site 1209 were generated, we observed long-term reproducibility in a liquid consistency standard (interrun precision, 1s, $n = 250$) to be 0.051, 0.018, and 0.023 mmol/mol for Mg/Ca, Sr/Ca, and Mn/Ca, respectively. During the same period, we observed long-term reproducibility in a foraminiferal consistency standard (interrun precision, 1s, $n = 35$) to be 0.252, 0.025, and 0.004 mmol/mol for Mg/Ca, Sr/Ca, and Mn/Ca, respectively. See (*43*).
22. The fragmentation index represents the percentage of fragments or partial to whole shells. Once dried, samples were sieved to isolate specimens >125 μm. About 300 specimens were then counted and identified as perfect planktonic, fragmented planktonic, and benthic foraminifera, as well as pyrite grains and fish debris. Several samples were then recounted to ensure reproducibility. $\%CaCO_3$ was determined by the coulometric method. External precision based on replicates is $\pm 1.5\%$.
23. U. Röhl, T. J. Bralower, R. D. Norris, G. Wefer, *Geology* **28**, 927 (2000).
24. K. A. Farley, S. F. Eltgroth, *Earth Planet. Sci. Lett.* **208**, 135 (2003).
25. D. Nürnberg, J. Bijma, C. Hemleben, *Geochim. Cosmochim. Acta* **60**, 803 (1996).
26. P. S. Dekens, D. W. Lea, D. K. Pak, H. J. Spero, *Geochem. Geophys. Geosyst.* **3** (4), 10.1029/2001GC000200 (2002).
27. P. Anand, H. Elderfield, M. H. Conte, *Paleoceanography* **18**, 1050 (2003).
28. Y. Rosenthal, G. P. Lohmann, *Paleoceanography* **17**, 1044 (2002).
29. J. Erez, B. Luz, *Geochim. Cosmochim. Acta* **47**, 1025 (1983).
30. Y. Bouvier-Soumagnac, J. C. Duplessy, *J. Foraminiferal Res.* **15**, 302 (1985).
31. Here we assume that continental ice sheets, if present on Antarctica, are of insufficient mass to noticeably affect mean ocean $\delta^{18}O$. Currently, the lack of sediment cores or outcrops of this age from the Antarctic margin, however, preclude a more definitive resolution to this issue.
32. D. P. Schrag, D. J. dePaolo, F. M. Richter, *Geochem. Cosmochem. Acta* **59**, 2265 (1995).
33. Y. Rosenthal, G. P. Lohmann, K. C. Lohmann, R. M. Sherrell, *Paleoceanography* **15**, 135 (2000).
34. J. C. Zachos, L. D. Stott, K. C. Lohmann, *Paleoceanography* **9**, 353 (1994).
35. H. J. Spero, J. Bijma, D. W. Lea, B. E. Bemis, *Nature* **390**, 497 (1997).
36. R. E. Zeebe, *Palaeogeogr. Palaeoclimatolo. Palaeoecol.* **170**, 49 (2001).
37. K. Billups, D. P. Schrag, *Earth Planet. Sci. Lett.* **209**, 181 (2003).
38. G. R. Dickens, *Bull. Soc. Géol. France* **171**, 37 (2000).
39. D. L. Royer *et al.*, *Science* **292**, 2310 (2001).
40. L. C. Sloan, M. Huber, A. Ewing, in *Reconstructing Ocean History: A Window into the Future*, F. Abrantes, A. Mix, Eds. (Kluwer Academic, New York, 1999), pp. 273–293.
41. G. A. Schmidt, D. T. Shindell, *Paleoceanography* **18**, 1004 (2003).
42. D. J. Thomas, J. C. Zachos, T. J. Bralower, E. Thomas, S. Bohaty, *Geology* **30**, 1067 (2002).
43. M. W. Wara *et al.*, *Geochem., Geophys., Geosyst.* **4**, 8406 (2003).

44. We thank B. Becker, R. Franks, S. Keller, H Leong, and O. Daignieres for technical support, and P. Koch, C. Shellito, L. Sloan, and M. Huber for their comments. The Ocean Drilling Program furnished samples. This research was supported by NSF grants EAR-9814833 and EAR-0120727.

Supporting Online Material

www.sciencemag.org/cgi/content/full/1090110/DC1
SOM Text
Figs. S1 and S2
Table S1
References

5 August 2003; accepted 15 October 2003
Published online 23 October 2003;
10.1126/science.1090110
Include this information when citing this paper.

Carbon in Amazon Forests: Unexpected Seasonal Fluxes and Disturbance-Induced Losses

Scott R. Saleska,[1]* Scott D. Miller,[2] Daniel M. Matross,[1] Michael L. Goulden,[2] Steven C. Wofsy,[1] Humberto R. da Rocha,[3] Plinio B. de Camargo,[4] Patrick Crill,[5]† Bruce C. Daube,[1] Helber C. de Freitas,[3] Lucy Hutyra,[1] Michael Keller,[5,6] Volker Kirchhoff,[7] Mary Menton,[2] J. William Munger,[1] Elizabeth Hammond Pyle,[1] Amy H. Rice,[1] Hudson Silva[5]

The net ecosystem exchange of carbon dioxide was measured by eddy covariance methods for 3 years in two old-growth forest sites near Santarém, Brazil. Carbon was lost in the wet season and gained in the dry season, which was opposite to the seasonal cycles of both tree growth and model predictions. The 3-year average carbon loss was 1.3 (confidence interval: 0.0 to 2.0) megagrams of carbon per hectare per year. Biometric observations confirmed the net loss but imply that it is a transient effect of recent disturbance superimposed on long-term balance. Given that episodic disturbances are characteristic of old-growth forests, it is likely that carbon sequestration is lower than has been inferred from recent eddy covariance studies at undisturbed sites.

The terrestrial biosphere currently sequesters 20 to 30% of global anthropogenic CO_2 emissions (*1*, *2*). Amazônia has been suggested to be a major contributor to observed interannual variations in this sink (*3*). The underlying causes are unclear. One hypothesis suggests that C uptake in old-growth Amazonian forests may be stimulated by rising atmospheric CO_2 (*4*–*7*). Also, water availability limits tree growth, potentially reducing C uptake in dry periods (*4*, *8*). Thus, in El Niño years, when much of Amazônia experiences low rainfall (*9*), old-growth forests could release CO_2 (*10*), a notable problem if El Niño frequency increases in future climates (*11*).

Evidence for uptake of 0.1 to 0.5 Mg C ha^{-1} $year^{-1}$ of CO_2 has been inferred from long-term tree data on forest plots (*12*, *13*), which is consistent with hypothetical CO_2 fertilization (*4*) but remains controversial (*14*, *15*). A surprisingly large uptake (1.0 to 5.9 Mg C ha^{-1} $year^{-1}$) (*16*–*19*) was inferred from several eddy covariance studies in Amazonian forests, much greater than the accumulation rates pre-

[1]Department of Earth and Planetary Sciences, Harvard University, Cambridge, MA 02138, USA. [2]University of California, Department of Earth System Science, Irvine, CA 92697, USA. [3]Department of Atmospheric Sciences, University of Sao Paulo, Sao Paulo 05508–900, Brazil. [4]Centro de Energia Nuclear na Agricultura, University of Sao Paulo, Piracicaba 13416–000, Brazil. [5]Complex Systems Research Center, University of New Hampshire, Durham, NH 03824, USA. [6]U.S. Department of Agriculture Forest Service, International Institute of Tropical Forestry, San Juan, PR 00926, USA. [7]Instituto Nacional De Pesquisas Espaciais (INPE), Sao Paulo 12227–010, Brazil.

*To whom correspondence should be addressed. E-mail: saleska@fas.harvard.edu
†Present address: Department of Geology and Geochemistry, Stockholm University, Stockholm 10691, Sweden.

dicted for CO_2 enrichment or observed in trees (*12*) and soils (*20*). If it were representative of Amazônia (*16*, *21*, *22*), the associated sink in undisturbed forests would be 0.5 to 3.0 Pg C $year^{-1}$, comparable to global terrestrial C uptake and inconsistent with atmospheric inversion studies (*3*). It is possible that loss processes [deforestation (*23*) and evasion of CO_2 from rivers (*24*)] are larger than previously thought, or flux sites could have selectively avoided locations affected by disturbance, missing associated C losses (*25*, *26*). Alternatively, the flux studies may have overestimated uptake.

We measured C exchange for two old-growth Amazonian forests in the Tapajós National Forest near km 67 (02°51′S, 54°58′W) (*27*) and km 83 (03°03′S, 54°56′W) (*28*–*30*) of the Santarém-Cuiabá highway, just south of Santarém, Pará, Brazil, using eddy covariance methods (*31*). The site receives 1920 mm $year^{-1}$ of rainfall and has a 7-month wet season (months with >100 mm of precipitation), representing the 25th to 30th percentile of each metric among Amazon forests (fig. S2). Moist tropical forests like the Tapajós, which are drier than the more extensive wet forests, may be models for the future Amazon (which is predicted to become drier with climate change) (*10*, *11*).

We simultaneously tracked changes in the forest structure and monitored C that was stored in live wood (resulting from tree recruitment, growth, and mortality) and dead wood (resulting from tree mortality inputs and respiration losses) by means of biometric observations at km 67 (*32*). Long-term rates of C storage were determined by comparing inventories from 1984 and 2000 at km 83 (*33*). Thus, we independently checked C balances that had been inferred from flux data and studied the processes mediating C uptake and loss.

Eddy covariance data from the two sites together cover 1 July 2000 to 1 August 2003 nearly continuously. Hourly data for net ecosystem exchange (NEE) (*34*) were obtained for 83% of 31,000 hours, including above-canopy fluxes and CO_2 storage within the canopy. Gaps were caused by calibrations, intense precipitation events, maintenance, and equipment faults. The two sites are well-suited for eddy covariance measurements, have similar weather (Fig. 1A), and exhibit a similar dependence of NEE on sunlight (Fig. 1B). NEE was underestimated during calm nighttime conditions at both sites (Fig. 1C); we applied corrections using procedures developed for mid-latitude forests and adapted, with rigorous testing, for Tapajós (*35*). Cumulative values for NEE were indistinguishable after applying this correction (fig. S7).

Carbon was taken up in the dry season and released in the wet season (Fig. 2A), opposite to seasonal variations for non–El Niño years in two ecosystem models (*36*, *37*) (Fig. 2A) and inverse to the seasonality observed for tree growth (Fig. 2C). Seasonal precipitation patterns were very similar in models and observations (Fig. 2D), indicating that the discrepancy is likely mechanistic rather than reflective of differences in environmental forcing.

Seasonal variations in NEE reflect the influence of moisture and sunlight on photosynthesis and respiration. Photosynthesis [gross ecosystem production (GEP) (*38*)] responded weakly to seasonal changes in precipitation, but respiration responded strongly, with the peak wet-season month (March) 40% higher than the minimum dry-season month (November) (Fig. 2B) (*39*). The models, however, predicted that GEP was water-limited and thus more sensitive to precipitation than respiration (*36*, *37*). Trees in the Tapajós access deep soil water during dry periods and show little evidence of stress (*29*, *40*); rates for wood increment decline in the dry season, but remain substantial and notably increase just before rains return (Fig. 2C), suggesting an adaptive mechanism rather than a response to seasonal forcing (*30*). In contrast, respiration in soils, litter, and coarse woody debris (CWD) is concentrated near the surface and consequently inhibited by desiccation during the dry season (Fig. 2C) (*30*).

Seasonal variation of NEE was stronger in Tapajós (700 kg C ha^{-1} $month^{-1}$ minimum to maximum) (Fig. 2A) than in forests near Manaus to the west (*17*, *41*) (~150 kg C ha^{-1} $month^{-1}$ minimum to maximum) (*41*), and it had the opposite phase. Little seasonality was observed at Caxiuanã to the east (*19*). These differences derive from the longer dry seasons at Tapajós (*42*), which desiccate detrital material and reduce respiration, a pattern also observed in temperate forests (*43*) and mesquite woodlands (*44*) during dry periods.

The seasonality of C exchange has two important implications. First, the same model constructs (such as tree rooting depth and surface-litter layer thickness) affect seasonal and interannual variations of C exchange. The models predict an annual net C loss during El Niño droughts (*4*, *8*), but if a drought increases tree mortality (*45*, *46*) while inhibiting respiration, C losses are more likely to occur after the rains return and the wood decomposition accelerates.

Second, seasonal variations are important in global inversion studies. In the wet season, deep convection transports surface air to the free troposphere, diluting the effect of ecosystem fluxes on the near-surface CO_2 observations used in global inversions (*47*) and masking any net release of CO_2 similar to that observed here. In contrast, dry season fluxes are manifest in near-surface observations used in global inversions. Thus, if the higher amplitude reversed phase of seasonal C exchange in drier forests such as the Tapajós dominates seasonal variation for Amazônia, inversions incorporating biosphere models that predict the wrong seasonal phase will overestimate Amazonian C uptake.

We derived annual C balances for Tapajós forests by integrating NEE data over the observation period. Cumulative losses to the

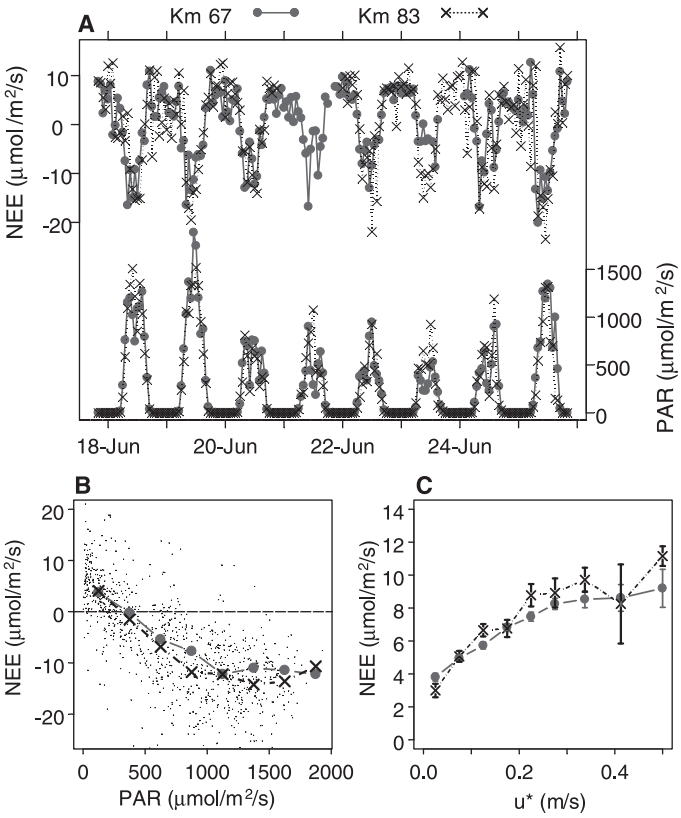

Fig. 1. Comparison between km 83 and km 67 tower sites. (**A**) Coherent time series for NEE and sunlight [photosynthetically active radiation (PAR)]. (**B**) Similar curves at the two sites for daytime NEE versus PAR. (**C**) Nighttime NEE versus friction velocity (u^*). Declining NEE at $u^* < 0.2$ is evidence that tower measurements underestimate NEE during calm conditions at night.

atmosphere were (0.0 to 1.9) ± 0.5, (0.5 to 2.3) ± 0.3, and (0.1 to 2.0) ± 0.3 Mg C ha^{-1} year^{-1} in year 1 (1 July 2000 to 1 July 2001 at km 83) and years 2 and 3 (1 July 2001 to 1 July 2003 at km 67), respectively (Fig. 3A). Uncertainties arise from two sources: corrections for nighttime underestimation of flux under conditions of low turbulence (represented by the range in parentheses) (*35*) and conventional statistical uncertainty [represented as ±95% confidence interval (CI)]. Nighttime corrections added 3.8 to 5.8 Mg C ha^{-1} year^{-1} at km 83, and 2.0 to 3.8 Mg C ha^{-1} year^{-1} at km 67, with bounds based on a conservative analysis of the dependence of apparent respiration rates on turbulence statistics (*35*). The greater prevalence of windy nights at km 67 resulted in smaller corrections for that site. Aggregating the different kinds of error and the errors across site years gave a mean loss of 1.3 (combined confidence interval: 0.0 to 2.3) Mg C ha^{-1} year^{-1} (Fig. 3B).

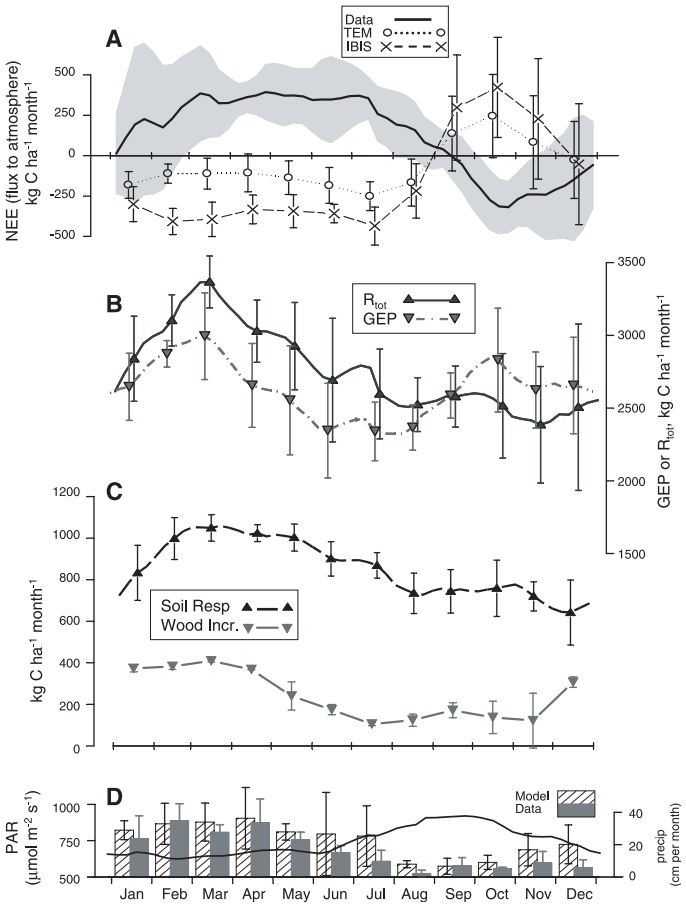

Fig. 2. (**A**) Tapajós National Forest average seasonal cycle of observed NEE is shown as a moving average monthly flux (solid curve) ± SD across 3 years (shaded area) from July 2000 to July 2003, and simulated NEE (error bars show ±SD across non–El Niño years from 1980 to 1995) is shown for the tower region with the TEM model (dotted curve) (*36*) and IBIS model (dashed curve) (*37*). (**B**) Average seasonal cycle of observed GEP (dashed curve) and whole-ecosystem respiration. R_{tot} (solid line) (*38*) was derived from NEE in (A). Error bars show ±SD, as in (A). (**C**) Average seasonal cycle of soil respiration (Soil Resp) is shown as a moving average monthly flux (±SD across 2 years, from April 2001 to April 2003). Average seasonal cycle of aboveground woody increment (Wood Incr.) is also shown (±SD across 2 years, from July 2000 to July 2002). Both cycles are from km 67 only. (**D**) Average seasonal cycle of observed PAR (solid curve, left *y* axis) and monthly precipitation (precip) (solid bars, right *y* axis) (bars show the mean, error bars show ±SD across years, from July 2000 to July 2003), together with model-input precipitation (hatched bars, error bars show ±SD). Model-index precipitation was composited from the same years as the model runs in (A).

Biometric observations at km 67 over an overlapping 2-year period also indicated a net loss of C (2.0 ± 1.6 Mg C ha^{-1} year^{-1}) (table S1) from above- and belowground pools of live and dead wood, with substantial contributions from respiration by notably large stocks of CWD. Generous allowance for C allocation to roots and to soil, within constraints from direct measurements of belowground root mass near the km 67 tower (*48*) and empirical studies of tropical soil C turnover (*20*), would not change the observation of net C loss (table S1 and Fig. 3B). Thus, biometric data support the carbon budget derived from eddy covariance data.

This is the first eddy covariance study in old-growth Amazonian rain forests that fails to indicate C sequestration. Had we not corrected for evident underestimation of nighttime fluxes, as has been done at most eddy flux sites worldwide (*49*), our measurements would indicate large uptake, comparable to previous Amazonian studies in which this correction was not applied (*18*, *19*). Our algorithm for correcting nighttime fluxes (*35*) is supported by biometric data, convergence of eddy flux results for the two towers using independent corrections, and entirely independent estimates of nighttime fluxes at km 67 using radon as a tracer (*50*). Notable uncertainties are associated with the nighttime flux correction, reflecting imperfect understanding of the details of canopy transport (*51*–*53*), but the available evidence (*49*) strongly suggests that uncorrected fluxes will overestimate uptake at most sites.

The respiration losses from the large stock of dead wood at km 67 exceeded the uptake of C by live biomass, despite high growth rates (*54*), reflecting disequilibrium of the vegetation assemblage (table S1A). Notably, the C was taken up mostly by small trees (table S1A), which also increased in stem density (4.8% recruitment into the >10-cm size class) (*55*, *56*). But no net long-term change in aboveground biomass was observed over the course of 16 years at km 83 (table S1B). We infer that the forest at km 67 is responding to a recent episode of high mortality, possibly triggered by drought associated with the strong El Niño events of the

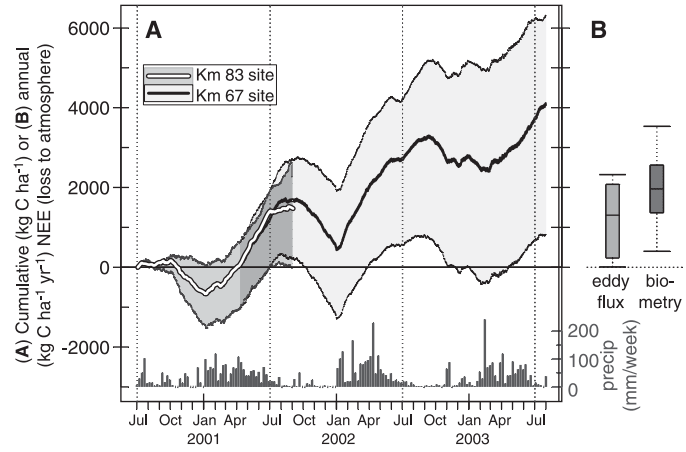

Fig. 3. (**A**) Cumulative NEE (white and black curves) at km 83 (1 July 2000 to 1 September 2001) and km 67 (10 April 2001 to 1 August 2003) with nighttime correction uncertainty (shaded area) (*35*). Dark gray shaded area is the period with data collection at both sites (10 April to 1 September 2001), before selective logging at km 83. The histogram along the bottom gives the average weekly precipitation from 1 July 2000 to 1 August 2003, measured at a location between the two towers (*48*). Vertical lines denote seasonal transitions (dry season is from about 1 July to 1 January). (**B**) Annual carbon balance, from eddy flux (1 July 2000 to 1 July 2003) and from short-term biometry (July 1999 to July 2001) (table S1). Potential bias errors (boxes), and 95% CI due to sampling uncertainty (error bars) are shown.

1990s (*57*). Dead trees were deposited on the forest floor, simultaneously opening canopy gaps that drive the current growth and recruitment of small trees.

The observations suggest that present C losses at km 67 are part of a cycle of disturbance and recovery superimposed on long-term balance and that substantial transient fluxes lag mortality events. Disturbance and recovery cycles, characterized by high C loss in the decade after disturbance followed by many decades of moderate uptake, may be inferred from the extensive ecological literature on disturbance dynamics (*58*) and have been predicted for old-growth Amazonian forests (*25*); the current study empirically quantifies the associated transient fluxes.

Episodic natural disturbances complicate estimates of regional C balance. If disturbance occurs on spatial scales larger than flux tower footprints or ecological plots, but smaller than landscape scales, most areas will be "recently undisturbed" and will take up C. But relatively rare "recently disturbed" areas will release C at rates sufficient to offset this uptake. Because study sites tend to avoid recent disturbance, regional C sequestration tends to be overestimated (*59*). Evidently, the disturbance history of study sites and the distribution of disturbance across the landscape (*25*) must be known to assess large-scale influences on the C budget, such as response to CO_2 fertilization.

Our results focus attention on the importance of respiration and disturbance for understanding the present and future C balance of Amazonian forests. The unexpected seasonality of C exchange, dominated by moisture effects on respiration, calls into question hypothesized C losses during El Niño–Southern Oscillation droughts and highlights the importance of using accurate seasonal fluxes for inverse atmospheric model studies. The observation of disturbance-induced loss implies that large-scale C balance depends critically on large-scale disturbance dynamics. Consequently, if study sites avoid recent disturbance, extrapolations to the whole basin will consistently overestimate C sequestration by Amazonian forests.

References and Notes

1. K. R. Gurney *et al.*, *Nature* **415**, 626 (2002).
2. R. F. Keeling, H. E. Garcia, *Proc. Natl. Acad. Sci. U.S.A.* **99**, 7848 (2002).
3. P. Bosquet *et al.*, *Science* **290**, 1342 (2000).
4. H. Tian *et al.*, *Nature* **396**, 664 (1998).
5. H. Tian *et al.*, *Global Ecol. Biogeogr.* **9**, 315 (2000).
6. I. C. Prentice, J. Lloyd, *Nature* **396**, 619 (1998).
7. C. Potter *et al.*, *J. Geophys. Res.* **106**, 10423 (2001).
8. A. Botta, N. Ramankutty, J. A. Foley, *Geophys. Res. Lett.* **29**, 1319 (2002).
9. C. F. Ropelewski, M. S. Halpert, *J. Climate* **2**, 268 (1989).
10. P. M. Cox *et al.*, *Nature* **408**, 184 (2000).
11. K. E. Trenberth, T. J. Hoar, *Geophys. Res. Lett.* **24**, 3057 (1997).
12. O. L. Phillips *et al.*, *Science* **282**, 439 (1998).
13. Y. Malhi *et al.*, *J. Veg. Sci*, **13**, 439 (2002).
14. D. A. Clark, *Ecol. Appl.* **12**, 3 (2002).
15. O. L. Phillips *et al.*, *Ecol. Appl.* **12**, 576 (2002).
16. J. Grace *et al.*, *Science* **270**, 778 (1995).
17. J. Grace *et al.*, *Global Change Biol.* **2**, 209 (1996).
18. Y. Mahli *et al.*, *J. Geophys Res.* **103**, 31593 (1998).
19. F. E. Carswell *et al.*, *J. Geophys. Res.* **107**, 8076 (2002).
20. E. D. C. Telles *et al.*, *Global Biogeochem. Cycles* **17**, 1040 (2003).
21. J. Grace, Y. Mahli, *Nature* **416**, 594 (2002).
22. M. O. Andreae *et al.*, *J. Geophys. Res.* **107**, 8066 (2002).
23. Y. Mahli, J. Grace, *Trends Ecol. Evol.* **15**, 332 (2000).
24. J. E. Ritchey, J. M. Melack, A. K. Aufdenkampe, V. M. Ballester, L. L. Hess, *Nature* **416**, 617 (2002).
25. P. R. Moorcroft, G. H. Hurtt, S. W. Pacala, *Ecol. Monogr.* **71**, 557 (2001).
26. M. Keller, D. A. Clark, D. B. Clark, A. M. Weitz, E. Veldkamp, *Science* **273**, 201 (1996).
27. A. H. Rice *et al.*, *Ecol. Appl.*, in press.
28. S. D. Miller *et al.*, *Ecol. Appl.*, in press.
29. H. R. Rocha *et al.*, *Ecol. Appl.*, in press.
30. M. L. Goulden, S. D. Miller, M. C. Menton, H. R. da Rocha, H. C. Freitas, *Ecol. Appl.*, in press.
31. Materials and methods are available as supporting material on *Science* Online.
32. For the km 67 biometry study (*27*, *49*) , we surveyed 20 ha of forest near the eddy-flux tower in July 1999 and resurveyed the same area in July 2001 (obtaining estimates of recruitment, growth, and mortality), including stocks of CWD. CWD respiration was calculated by applying density-specific respiration rates measured in the Amazon rainforest near Manaus to measured decay class–specific CWD mass at km 67 (*27*). Sampling uncertainty in all estimates was quantified using bootstrap analyses, with 95% CIs reported.
33. The km 83 long-term biometry study (*28*, *49*) compared a 1984 inventory of large trees (diameter at breast height $>$ 55 cm) in 48 ha around the eddy-flux tower location with an inventory of the same area in 2000 to analyze the change in large tree biomass. The measured small tree:large tree biomass ratio was used to estimate changes in smaller trees. Errors were quantified using a sensitivity analysis that bracketed a highly conservative range of plausible uncertainty. Flux contributions resulting from a change in CWD stocks over the period, which were not measured in the km 83 study, are likely much less important than in the km 67 study because of the long time between surveys (about twice the turnover time of CWD).
34. The NEE is the biotic flux from the forest, calculated as the sum of the eddy flux at the top of the canopy and the storage flux (the change in CO_2 stored in the canopy below the sensor).
35. We corrected for evident underestimation of nighttime NEE (Fig. 1C and figs. S4 and S5) by filtering out measurements taken during periods of weak mixing, indicated when u^* is below a given threshold (U^*_{thresh}), and replacing them with an estimate based on nearby NEE obtained during well-mixed conditions (when $u^* > U^*_{\mathrm{thresh}}$). Analysis (*49*) (figs. S4 and S5) indicated that a best-estimate U^*_{thresh} of $\sim$0.22 m sec^{-1} selects nighttime NEE measurements representative of total ecosystem respiration (these are 40 and 20% of total nighttime data at km 67 and km 83, respectively). We estimated a conservative uncertainty associated with this nighttime correction by calculating a low estimate for C balance using $U^*_{\mathrm{thresh}} = 0.17$ m s^{-1} and a high estimate using $U^*_{\mathrm{thresh}} = 0.30$ m s^{-1}. We believe that the probability of the true balance falling outside of this range is very small, but it is not rigorously quantifiable (*49*).
36. The Terrestrial Ecosystem Model (TEM) (*4*) is a highly aggregated box model. Results of model runs for the grid cell containing the towers are courtesy of J. Melillo and D. Kicklighter.
37. The Integrated Biosphere Simulator (IBIS) (*8*) is a mechanistic dynamic vegetation model that simulates interactions among different plant functional types. The current version includes multiple soil layers. Results of model runs for the grid cell containing the towers are courtesy of J. Foley, M. Costa, and A. Botta.
38. GEP represents the total photosynthetic production of the forest and is calculated as R_{tot} – NEE, where R_{tot} is total ecosystem respiration. R_{tot} equals NEE at night and is assumed to have the same average value during the day as at night. This method slightly underestimates the absolute value of GEP and R_{tot} (because higher daytime temperatures make daytime R_{tot} greater than nighttime NEE), but the relative seasonal pattern is not much affected. GEP is greater than net primary productivity, and R_{tot} is greater than heterotrophic respiration by the amount of autotrophic respiration.
39. Dry season decline in precipitation coincides with significant increases in other controlling variables at these sites, including photosynthetically active radiation, temperature, and vapor pressure deficit (VPD) (*29*), but the precipitation effect likely dominates; trends in VPD and photosynthetically active radiation have opposing effects on photosynthesis, whereas temperature increase would tend to increase dry-season respiration in the absence of water limitation.
40. D. Nepstad *et al.*, *Nature* **372**, 666 (1994).
41. A. C. Araujo *et al.*, *J. Geophys. Res.* **107**, 8090 (2002).
42. Mean number of months per year with $<$100 mm of rainfall (an indicator of dry-season intensity in tropical forests) was 4.7 (Tapajós), 2.4 (Manaus), and 2.8 months (Caxiuana) (*13*). The difference is stronger during the recent period of flux observations because the Manaus site experienced a wetter year and a wetter dry season than average during 1999 to 2000 (a La Niña period) when the seasonality there was strongest (*41*), whereas the Tapajós experienced close to average precipitation during the 2000 to 2003 measurements reported here. Though the Tapajós is somewhat drier than these other eddy flux sites, it does not represent the dry extreme [25 to 30% of the forested Amazon basin experiences equally dry or drier conditions (*49*) (fig. S2)].
43. K. E. Savage, E. A. Davidson, *Global Biogeochem. Cycles* **15**, 337 (2001).
44. R. L. Scott *et al.*, *Agric. For. Meteorol.*, in press.
45. R. Condit, S. P. Hubbell, R. B. Foster, *Ecol. Monogr.* **65**, 419 (1995).
46. G. B. Williamson *et al.*, *Conserv. Biol.* **14**, 1538 (2000).
47. S. Denning, I. Fung, D. Randall, *Nature* **376**, 240 (1995).
48. D. C. Nepstad *et al.*, *J. Geophys Res.* **107**, 8085 (2002).
49. Materials and methods are available as supporting material on *Science* Online.
50. C. Martens *et al.*, *Glob. Change Biol.*, in press.
51. X. Lee, *Agric. For. Meteorol.* **91**, 39 (1998).
52. R. K. Sakai, D. R. Fitzjarrald, K. E. Moore, *J. Appl. Meteorol.* **40**, 2178 (2001).
53. B. Kruijt *et al.*, *Ecol. Appl.*, in press.
54. Net uptake at km 67 in live biomass only (1.4 $\pm$ 0.6 Mg C ha^{-1} year^{-1}) (table S1A) is at the 90th percentile of uptake observed across all 68 tropical forest plots in (*12*).
55. Observed recruitment is high; long-term average recruitment rates in Amazonian permanent study plots were 0.8 to 2.8% (*56*).
56. O. L. Phillips, A. H. Gentry, *Science* **263**, 954 (1994).
57. M. J. McPhaden, *Nature* **398**, 559 (1999).
58. D. Scheil, D. F. Burslem, *Trends Ecol. Evol.* **18**, 18 (2003).
59. C. Körner, *Science* **300**, 1242 (2003).

60. This paper is a product of the Large-Scale Biosphere-Atmosphere Experiment in Amazonia (LBA), led by Brazil's Ministry of Science and Technology. Supported by NASA grants (LBA-ECO) to Harvard University (NCC5-341) and University of California, Irvine (NCC5-280); the Conselho Nacional de Desenvolvimento Cientifico; and the Harvard College Research Program. We thank D. Fitzjarrald, J. Foley, D. Kicklighter, J. Melillo, and A. Nobre for helpful comments and discussion; V. Y. Chow for analysis of precipitation data; B. Reed, L. Merry, D. Hodkinson, F. A. Leão, D. Amaral, and the staff of the LBA-Santarém Office for their extensive logistical support and patience; and N. de Souza Carvalho, E. Pedroso, and N. Rosa for botanical identifications.

Supporting Online Material

www.sciencemag.org/cgi/content/full/302/5650/1554/DC1

Materials and Methods

Figs. S1 to S7

Table S1

References and Notes

4 September 2003; accepted 16 October 2003